

Characteristics of slow and fast ion dynamics in a lithium metasilicate glass

Junko Habasaki

Department of Electronic Chemistry, Tokyo Institute of Technology, Nagatsuta 4259, Yokohama 226-8502, Japan

Yasuaki Hiwatari

Department of Computational Science, Faculty of Science, Kanazawa University, Kakuma, Kanazawa 920-1192, Japan

(Received 11 August 1998)

Molecular dynamics simulations of lithium metasilicate (Li_2SiO_3) glass have been performed. The motion of lithium ions is divided into slow (*A*) and fast (*B*) categories in the glassy state. The waiting time distribution of the jump motion of each component shows power law behavior with different exponents. Slow dynamics are caused by localized jump motions and the long waiting time. On the other hand, the fast dynamics of the lithium ions in Li_2SiO_3 are characterized as Lévy flight caused by cooperative jumps. Short intervals of jump events also occur in the fast dynamics in the short time region. Both the temporal and spatial terms contribute to the dynamics acceleration and the heterogeneity caused by these two kinds of dynamics is illustrated. The slow dynamics characteristics of the “glass transition” and in the “mixed alkali effect” are discussed. [S1063-651X(99)08406-8]

PACS number(s): 89.80.+h, 66.10.Ed, 66.30.Dn

I. INTRODUCTION

Dynamical processes in disordered media differ from simple Brownian motion. The slow dynamics characterized by a small γ' (<1) value of the mean square displacement (MSD) $\langle R^2(t) \rangle \sim t^{\gamma'}$ is usually observed near the glass transition temperature in many systems and is explained by the continuous time random walk (CTRW) method, which has been extended to the dynamics on fractal structures [1,2]. The slow dynamics is also characterized by a stretched exponential ($\sim A \exp[-(t/\tau)^\beta]$) decay (α relaxation). In our previous studies, small γ' values and small β (<1) values were observed for the motion of lithium ions in a lithium metasilicate glass [3,4]. Lithium ions showing single jumps were found to be localized due to a locally low dimensional path [4,5] and long waiting times also contributed to the slow dynamics of the component. The γ' and β values depended on the geometrical correlation of successive jumps and the waiting time distribution of the jump motions. Thus both spatial (geometrical) and temporal terms affect the γ' and β values. On the other hand, a component showing accelerated dynamics with $\gamma' > 1$ was found in the motion of Li ions. We have found that the cooperative jumps (simultaneous jumps of neighboring ions or occurring within several picoseconds before the relaxation of the jump sites) cause acceleration since the site needed for the backward jump of the first ion after a cooperative jump is already occupied by the second ion [4,5]. The fast dynamics has been characterized as a Lévy flight [2], since power law distribution of the displacements and that of the number of atoms participating in the cooperative jumps were observed [4,5]. These distributions are also related to the geometry of the jump motions. In the present work, attention is focused on the temporal term of the accelerated dynamics to determine if the dynamics can be understood by an extended CTRW. Additional features of the dynamics such as heterogeneity were also examined. The roles of the temporal and spatial terms in the glass transition problem and in the “mixed alkali effect” [6–10] are dis-

cussed. Factors affecting the dynamics are important not only for the understanding of these glasses but also in the design of high conductivity materials.

II. MOLECULAR DYNAMICS SIMULATION

Molecular dynamics simulations were performed in the same way as in previous studies [3–5,9–13]. The numbers of particles in the basic cube were 144 Li, 72 Si, and 216 O of Li_2SiO_3 . The volume was fixed as that derived by an *NPT* (constant pressure and temperature) ensemble simulation. The glass transition temperature was approximately 830 K. Pair potential functions of the Gilbert-Ida type [14] and r^{-6} terms were used. The parameters of the potentials used were previously derived on the basis of *ab initio* molecular orbital calculations [13] and their validity was checked in the liquid, glassy, and crystal states under constant pressure conditions. A run, up to 1 ns (250 000 steps), was performed for the Li_2SiO_3 system [4,5] at 700 K.

Analysis of the jump motion

The number of jumps for each ion were counted. Displacement greater than 1/2 of the distance of the first maximum of the pair correlation function $g(r)_{\text{Li-Li}}$ was taken as a jump, with the atom coordinates averaged over several picoseconds to remove the effect of small displacements [3]. The particles showing a squared displacement less than the squared distance at the first minimum of $g(r)_{\text{Li-Li}}$ are defined as type *A*. Namely, the ion is located within neighboring sites during a given time *T*. Particles showing a squared displacement greater than the squared distance at the first minimum of $g(r)_{\text{Li-Li}}$ are defined as type *B* and contribute to the long time dynamics. Two kinds of definitions of type *A* and *B* are used in this work since the difference of *A* and *B* depends on the *T* and time windows used. In definition I, a time window is not used and $T = 1$ ns. (This definition is the same as that used in previous work [4].) The number of particles of types *A* and *B* were 76 and 68, respectively. In definition II, a time

window of 80 ps (100 points of initial t) is used and types A and B are distinguished by the values of the averaged squared displacement over 920 ps. With this definition, the number of particles of A and B types were 85 and 59, respectively. The differences caused by these definitions will be discussed later. The time window used in the definition II was not so wide as to hide dynamic heterogeneity in the glass.

III. RESULTS AND DISCUSSION

A. Separation of time and space aspects

In previous works on Li_2SiO_3 [4,5,11], the dynamics of the lithium ions were found to divide into two types in the glassy state. The plot of displacements of Li ions against jump angles between successive jumps (measured using a fixed scale during 1 ns at 700 K) showed clearly two regions (cf. Fig. 6 in [4]). The component around $\theta/2\pi=0.2$ meant a larger forward correlation probability of jumps, while the component at around $\theta/2\pi=0.5$ indicated a larger back correlation probability of jumps. Since many particles keep their characteristics for a fairly long time in a glassy state, we have divided the particles into types A (slow dynamics) and B (fast dynamics). Type A particles are located within neighboring sites during a 1-ns run and therefore do not contribute to diffusion or the dc but can contribute to the ac. Such particles show only single jumps and tend to return to their original sites due to low dimensional local paths. On the other hand, type B particles can go to second neighboring sites or to further sites by cooperative jump motions and thereby contribute to the long time diffusive dynamics by using three dimensional jump paths [4]. This situation differs from that in the liquid state where no particle can be localized for a long period. The type B dynamics also differs from that in the liquid state, where the motion of particles can be usually described by Gaussian dynamics. Since displacements of particles show a power law distribution in the longer r region, the accelerated dynamics caused by the cooperative jumps was characterized as a Lévy flight [2]. We plan to discuss the non-Gaussian character of such motion elsewhere. The large forward correlation probability (restricted angles of jump motion) and the power law distribution of characteristic jump lengths for the jump motions are the criteria of the Lévy flight dynamics. Mean square displacements $R^2(t)$ of types A and B are shown in Fig. 1. Here the values are averaged using a time window of 80 ps for smoothing (definition II). In a similar plot in our previous work [4], the squared displacements were averaged only for the particle numbers and that result was for a given t_0 value (definition I). Use of a larger time window diminishes the statistical error; however, differences of types A and B be-

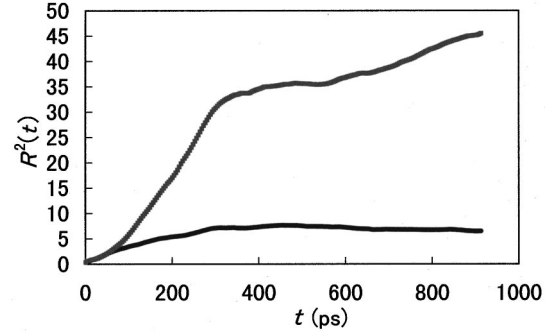


FIG. 1. Mean squared displacements of Li ions in Li_2SiO_3 for types A and B at 700 K: A , lower curve; B , upper curve.

come unclear due to the exchange between localized motion and diffusive motion. In a previous paper [11] we proposed a method to separate the time and space exponents in the MSD, which is applied here to analyze the characteristics of types A and B . The slopes thus obtained, in the region from 50 to 300 ps, are given in Table I for both definitions. A temporal term was obtained by plotting the accumulated number of jumps against time. Here, by definition I, the slope for the temporal term of the type A ion was about 1, while that of the spatial term was smaller than 1. Therefore, the behavior of these type A ions in this time region is mainly characterized by a geometric factor (backward correlation of the jump motion). On the other hand, the slopes of type B ions for spatial and temporal terms are greater than 1. This means that the acceleration is related to both terms. These distinctions are still clear using definition II.

B. Waiting time distribution

The large slopes for the space terms, shown in Table I, for type component B ions can be explained by the forward correlated motion of successive jumps caused by cooperative jumps. The large slope (larger than 1) of the time dependent term of type B ions means that the jump interval of the successive jumps tends to be shorter than the previous jump interval. Some examples of the time development of displacements of type B Li ions during 1 ns are shown in Fig. 2. The time interval between jumps seems to become shorter when the successive jumps occur (for example, see the 100–400 ps region of the top and next to the top cases in Fig. 2). To confirm these characteristics the distribution of jump intervals for types A and B during 1 ns were plotted (Fig. 3). The log-log plot was linear. That is, $\phi(t)$, the probability of the interjump intervals, has the probability

$$\phi(t) \sim at^{-(\gamma+1)}. \quad (1)$$

The slopes for types A and B using definition I were -1.87 ($\gamma=0.87$) and -2.13 ($\gamma=1.13$), respectively. These

TABLE I. Contribution of temporal and spatial parts to the MSD in Li_2SiO_3 in the region 50–300 ps.

Definition	Component	Slope	$\log_{10}N/\log_{10}(t/\text{ps})$	$\log_{10}(R^2/\text{Å}^2)/\log_{10}N$	$\log_{10}(R^2/\text{Å}^2)/\log_{10}(t/\text{ps})$
I	A		1.15	0.55	0.64
	B		1.47	1.20	1.77
II	A		1.03	0.66	0.68
	B		1.30	1.19	1.55

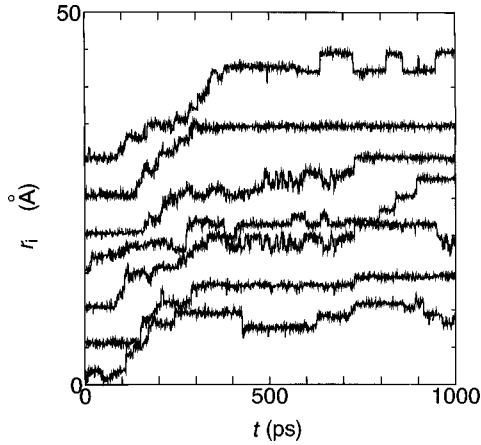


FIG. 2. Displacements of seven Li ions with large motion in Li_2SiO_3 at 700 K.

results mean that long time intervals are frequently observed for the localized component, whereas short time intervals are frequently observed for the diffusive component. The mean waiting time of the jump motion $\langle t \rangle$ is usually defined by

$$\langle t \rangle = \int_0^{\infty} t' \phi(t') dt' \quad (2)$$

and $N(T)$ (the number of jumps accumulated until T) is obtained from $T/\langle t \rangle$. Thus $N(t)$ is related to $\phi(t)$. Wang [15] has discussed the importance of a stochastic function $U(t)$, which is the total number of “jump” events in $(0, t)$ in Lévy motion [the Klafter-Blumen-Shlesinger (KBS) model [16]], where straight motion steps of particles are interrupted by jumps. By “jump” he means a scattering event when the direction of velocity is chosen anew. Therefore, the physical meaning of the jump differs from that in our flight motion

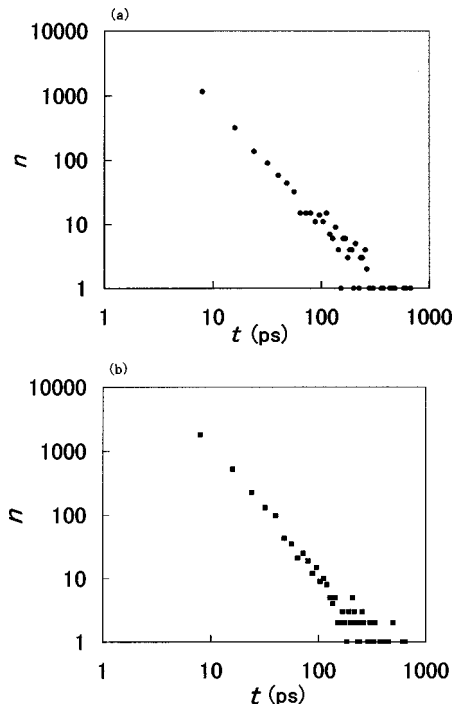


FIG. 3. Distribution of the jump intervals during 1 ns for types (a) A and (b) B.

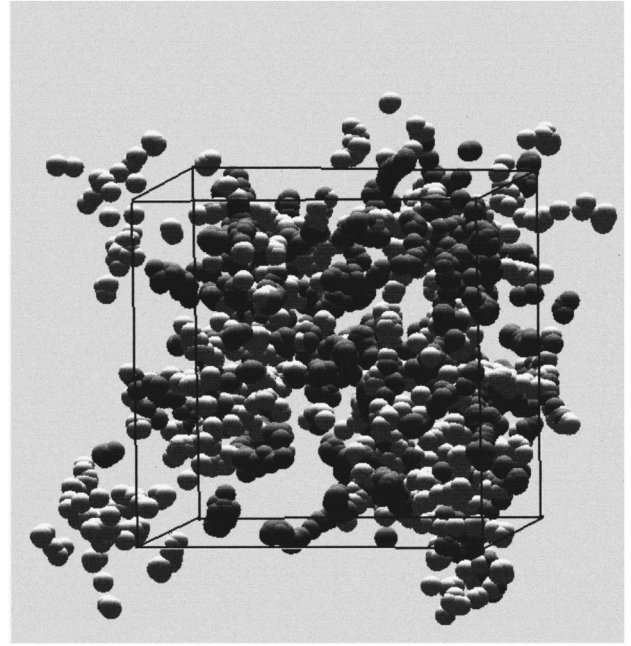


FIG. 4. Mean positions of particles of types A and B during a 1-ns run plotted every 100 ps. A, gray; B, white.

where long jumps are interrupted by trapping. However, if we neglect the geometrical term, $\langle U(t) \rangle$ is directly related to the mean square displacement and the role of $U(t)$ is the same as that of $N(t)$, in spite of the different physical meanings. Thus the discussion about $U(t)$ will be applicable to $N(t)$,

$$N(t) = \int_0^t Z(t') dt', \quad (3)$$

where $Z(t)$ is the indicator function for the jump event. The long time limit of $\langle N(t) \rangle / t$ is a measure of the intermittency of the dynamics as introduced for the turbulent flow by Townsend [17]. The $N(t)$ ($t \rightarrow \infty$) for different values of γ is known to be [15]

$$\langle N(t) \rangle \sim \begin{cases} (\sin \gamma \pi / A \gamma \pi) t^\gamma, & \gamma < 1 \\ \frac{t}{A \ln(t/A)}, & \gamma = 1 \\ t / (1 + \tau_1), & \gamma > 1. \end{cases} \quad (4)$$

When $\gamma < 1$ the fractal time is as usually observed in the slow dynamics in glasses. The trapping diffusion model [18] successfully explains the glass transition of fragile glasses such as soft core glass, where the power law distribution of the waiting time is observed.

In a glassy state, the first moment of the waiting time distribution is infinite. In the case with $\gamma < 1$, regenerative events occur on a random subset in time. This overcomes the divergence of the dynamics and time dependent character will be observed (the probability of jump motion decreases and vanishes in the longer t limit). On the other hand, the mean waiting time in the case of $\gamma > 1$ (it may be described also as fractal time in a broad sense) is finite. In such a case, the long time behavior of the dynamics is expected to be

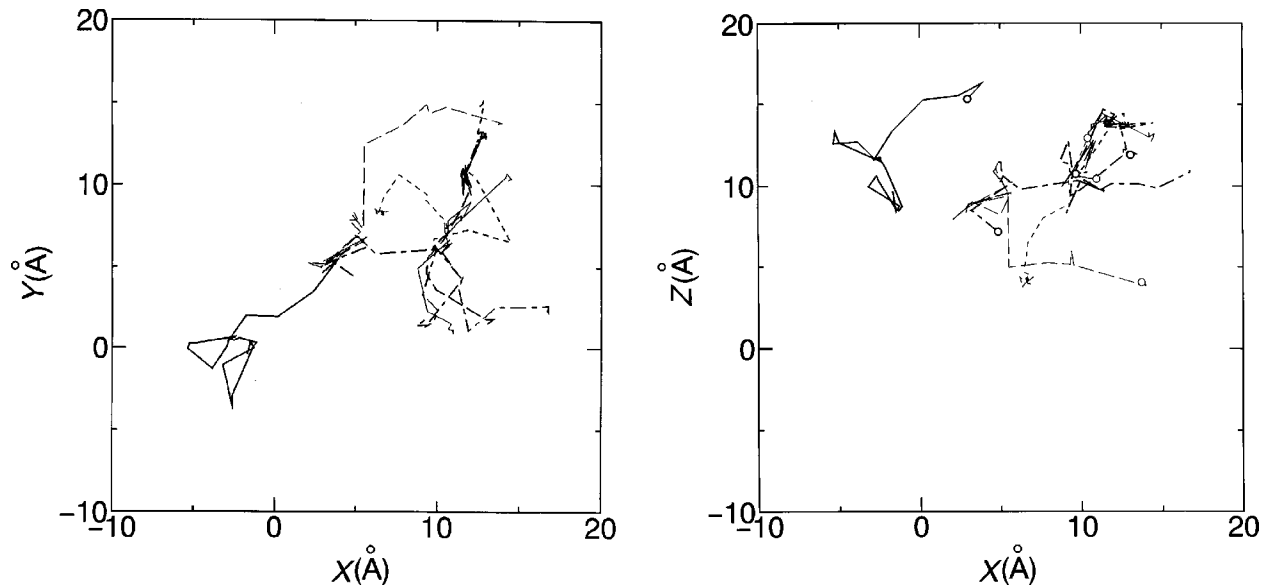


FIG. 5. x - y and x - z projections of the trajectories of the seven Li ions with large motions during a 1-ns run. The ions correspond to those in Fig. 2.

come independent of time and to be a Debye type [2,15]. If the mean waiting time $\langle t \rangle$ is regarded as a constant, then $N(t)$ should increase linearly even in a short time region. However, the slope in the log-log plot of N against t in Table I for type B ions is greater than 1. This means that the waiting time of the jump is a function of time in the observed time region. In the present system, the acceleration of jump interval is considered as the cause of the waiting time distribution of $\gamma > 1$. Namely, the next jump motion happens more quickly as a result of the previous jump (due to cooperative jumps) and the waiting time distribution with $\gamma > 1$ consists of time dependent subsets. When the mean waiting time behaves as $\sim A + t^{-\beta'}$ in a limited time region (where A is a constant), $N(t)$ becomes $\sim t^{1+\beta'}$. Thus the acceleration of the dynamics is caused not only by the forward correlated jumps but also by the change in frequency of jump events in a short time region. In the KBS model [16], the Lévy flight is connected to a fractal time with $\gamma < 1$. In the present system, the power distribution of the characteristic length of jump motions is not coupled with a fractal time with $\gamma < 1$. The mixed alkali effect (the large decrease in ion dynamics in the mixed alkali glasses) [6–8] is another example of the slow dynamics in a glass. The slowing down of the diffusion of alkali metal ions in LiKSIO_3 were explained by the blockage of cooperative jumps by the interception of the jump paths of different kinds of alkali ions [5,9–12,19]. In contrast with the glass transition described by the trapping diffusion model, where the waiting time distribution plays a dominant role in determining the dynamics, the change in the geometrical term plays an important role in the mixed alkali effect.

C. Heterogeneity of the dynamics

An illustration of the trajectories of particles of type A and B ions using definition I is shown in Fig. 4, where the mean positions of Li ions in every 100 ps during 1 ns are plotted. In some small regions, types A and B seem to mix with each other; however, in other regions, no mixing occurs. The het-

erogeneity of the dynamics held for a fairly long time (\sim ns), thus both types keep their characteristics up to the nanosecond regions. The total jump path has three dimensional connections, as already mentioned in a previous paper [12]; however, the region for component B has lower dimension. That is, the effective conduction path is low dimensional due to the large forward correlations in the cooperative jump motions. The trajectories of seven particles, which show large displacements during 1 ns, projected onto the x - y and x - z planes for type B are shown in Fig. 5 and can be seen to overlap each other. This means that a common path of these particles exists. Silicate glasses with high lithium contents are known as materials of high conductivity. Low dimensional motion in high dimensional paths should play a role in the effective transport.

IV. CONCLUSION

Some characteristics of the slow and fast dynamics in a metasilicate glass have been examined. Both the slowing down and acceleration of the jump motion were related to both space and time terms. A large forward correlation probability and shorter time intervals of the jumps due to cooperative jumps accelerate the dynamics of the lithium ions. By contrast, the large back correlation probability and the long time intervals of single jumps cause slowing down of the dynamics near the glass transition region. Thus there are two possible mechanisms to accelerate the jump diffusion. One is to change the geometrical nature of the jump paths and motions. The other is to change the temporal character of the jump. The cooperative motion of like ions plays a role accelerating both factors in the lithium metasilicate system.

ACKNOWLEDGMENTS

Some of the calculations in this work were performed using the SX-3/34R computer at the Institute for Molecular Science in Okazaki. The CPU time made available to us is gratefully acknowledged.

- [1] A. Blumen, K. Klafter, B. S. White, and G. Zumofen, *Phys. Rev. Lett.* **53**, 1301 (1984), and references herein.
- [2] M. F. Shlesinger, G. M. Zaslavsky, and J. Klafter, *Nature (London)* **363**, 31 (1993); J. Klafter, M. F. Shlesinger, and G. Zumofen, *Phys. Today* **49**(2), 33 (1996).
- [3] J. Habasaki, I. Okada, and Y. Hiwatari, *Phys. Rev. E* **52**, 2681 (1995).
- [4] J. Habasaki, I. Okada, and Y. Hiwatari, *Phys. Rev. B* **55**, 6309 (1997).
- [5] J. Habasaki, I. Okada, and Y. Hiwatari, in *Structure and Dynamics of Glasses and Glass Formers*, edited by C. A. Angell, K. L. Ngai, J. Kieffer, T. Egami, and G. U. Nienhaus, MRS Symposia Proceedings No. 455 (Materials Research Society, Pittsburgh, 1997), p. 91.
- [6] J. O. Isard, *J. Non-Cryst. Solids* **1**, 235 (1969).
- [7] D. E. Day, *J. Non-Cryst. Solids* **21**, 343 (1976).
- [8] M. D. Ingram, *Phys. Chem. Glasses* **28**, 215 (1987).
- [9] J. Habasaki, I. Okada, and Y. Hiwatari, *J. Non-Cryst. Solids* **183**, 12 (1995).
- [10] J. Habasaki, I. Okada, and Y. Hiwatari, *J. Non-Cryst. Solids* **208**, 181 (1996).
- [11] J. Habasaki, I. Okada, and Y. Hiwatari, *J. Phys. Soc. Jpn.* **67**, 2012 (1998).
- [12] J. Habasaki, I. Okada, and Y. Hiwatari, *Prog. Theor. Phys.-Suppl.* **126**, 399 (1997).
- [13] J. Habasaki and I. Okada, *Mol. Simul.* **9**, 319 (1992).
- [14] Y. Ida, *Phys. Earth Planet. Inter.* **13**, 97 (1976).
- [15] X.-J. Wang, *Phys. Rev. A* **45**, 8407 (1992).
- [16] J. Klafter, A. Blumen, and M. F. Shlesinger, *Phys. Rev. A* **35**, 3081 (1987).
- [17] A. A. Townsend, *Aust. J. Sci. Res. Ser. A* **1**, 161 (1948).
- [18] T. Odagaki and Y. Hiwatari, *Phys. Rev. A* **41**, 929 (1990).
- [19] S. Balasubramanian and K. J. Rao, *J. Phys. Chem.* **97**, 8835 (1993); *J. Non-Cryst. Solids* **181**, 157 (1995).